ASTR

ORIGINAL ARTICLE
pISSN 2288-6575 • eISSN 2288-6796
https://doi.org/10.4174/astr.2025.108.3.186
Annals of Surgical Treatment and Research

Scaffold implantation vs. intravenous delivery: a comparative preclinical animal study evaluating peroxisome proliferator-activated receptor gamma coactivator 1-alpha adipose-derived stem cells in liver fibrosis treatment

Joseph Ahn[1], Jung Hyun Park[2,3], Ho Joong Choi[4], Dosang Lee[3,4], Ha-Eun Hong[3,5], Ok-Hee Kim[3,5], Say-June Kim[3,4,5]

[1]Department of Surgery, Bundang Jesaeng General Hospital, Seongnam, Korea
[2]Department of Surgery, Eunpyeong St. Mary's Hospital, College of Medicine, The Catholic University of Korea, Seoul, Korea
[3]Catholic Central Laboratory of Surgery, College of Medicine, The Catholic University of Korea, Seoul, Korea
[4]Department of Surgery, Seoul St. Mary's Hospital, College of Medicine, The Catholic University of Korea, Seoul, Korea
[5]Translational Research Team, Surginex Co., Ltd., Seoul, Korea

Purpose: Regenerative medicine is expected to offer an alternative to liver transplantation for treating liver diseases in the future, with one significant challenge being the establishment of an effective stem cell administration route. This study assessed the antifibrogenic effects of adipose-derived stem cells (ASCs) in a liver fibrosis mouse model, focusing on 2 methods of delivery: intravenous injection and scaffold implantation.
Methods: An extracellular matrix mimic scaffold was utilized for culturing peroxisome proliferator-activated receptor gamma coactivator 1-alpha–overexpressing ASCs (tASCs). These scaffolds, laden with tASCs, were then implanted subcutaneously in mice exhibiting liver fibrosis. In contrast, the Cell groups received biweekly intravenous injections of tASCs for 4 weeks. After 4 weeks, tissue samples were harvested from the euthanized mice for subsequent analysis.
Results: Real-time PCR and Western blot analyses on liver tissues, focusing on markers like alpha-smooth muscle actin (α-SMA), matrix metalloproteinase-2, and transforming growth factor-beta 1 (TGF-β1), showed that both delivery routes substantially lowered fibrotic and inflammatory markers compared to controls ($P < 0.05$), with no significant differences between the routes. Histological examinations, along with immunohistochemical analysis of α-SMA, collagen type I alpha, and TGF-β1, revealed that the scaffold implantation approach resulted in a greater reduction in fibrosis and lower immunoreactivity for fibrotic markers than intravenous delivery ($P < 0.05$).
Conclusion: These findings indicate that delivering tASCs via a scaffold could be more effective, or at least similarly effective, in treating liver fibrosis compared to intravenous delivery. Scaffold implantation could offer a beneficial alternative to frequent intravenous treatments, suggesting its potential utility in clinical applications for liver disease treatment.
[Ann Surg Treat Res 2025;108(3):186-197]

Key Words: Adipose-derived mesenchymal stem cells, Extracellular matrix, Liver fibrosis, Peroxisome proliferator-activated receptor gamma coactivator 1-alpha, Tissue scaffolds

Received July 18, 2024, **Revised** September 30, 2024, **Accepted** November 25, 2024

Corresponding Author: Say-June Kim
Division of Hepatobiliary Pancreatic Surgery, Department of Surgery, Seoul St. Mary's Hospital, College of Medicine, The Catholic University of Korea, 222 Banpo-daero, Seocho-gu, Seoul 06591, Korea.
Tel: +82-2-3147-8835, **Fax:** +82-2-535-0070
E-mail: sayjunekim@catholic.ac.kr
ORCID: https://orcid.org/0000-0001-5171-4837

INTRODUCTION

In recent decades, liver diseases have become a significant global health concern, contributing to increasing rates of mortality and morbidity, often leading to end-stage liver disease (ESLD). Currently, liver transplantation is the primary treatment for ESLD. However, the complexity of the transplant procedure and the shortage of available donor organs limit this option to only a small number of patients, emphasizing the need for novel therapeutic approaches [1,2]. Regenerative medicine, particularly liver-targeted cell-based therapies, has gained attention as an important research area, focusing on hepatocytes, mesenchymal stromal cells, and macrophages [3]. Although these therapies have been increasingly tested in clinical trials, evidence supporting their clinical efficacy remains sparse, and their long-term effects are not yet fully understood, highlighting the urgent demand for innovative advancements in this field.

A pivotal aspect of liver diseases and failure is the route of administration of cell therapies, which determines cell engraftment and function post-transplantation. Several protocols aimed at enhancing the efficacy of cell transplantation have been proposed, such as (1) intravascular delivery through the portal vein, hepatic artery, or splenic artery, and (2) direct intrahepatic or intrasplenic injection. However, these methods have proven to be challenging and yielded disappointing results [4-6]. To overcome these limitations, the utilization of bioactive scaffolds has emerged as a significant advancement in cell therapy for liver diseases, crucially aiding in stimulating cell growth and differentiation [7,8]. These scaffolds adeptly mimic the liver's extracellular matrix (ECM), providing a conducive environment for effective liver tissue reconstruction. This advancement represents a significant leap forward in regenerative medicine, offering a promising avenue for treating liver diseases. Despite the growing focus on scaffold-based approaches in stem cell therapies for liver diseases, comparative studies between these methods and conventional intravenous delivery have not been sufficiently conducted. This study assessed the antifibrogenic effects of peroxisome proliferator-activated receptor gamma coactivator 1-alpha (PGC-1α)-overexpressing adipose-derived stem cells (tASCs) in a liver fibrosis mouse model, focusing on 2 methods of delivery: intravenous injection and scaffold implantation. The comparative results of this study are anticipated to provide crucial insights into the choice between stem cells' intravenous delivery *vs.* scaffold delivery.

METHODS

Cell culture

Human adipose-derived mesenchymal stem cells (ASCs) were obtained from Hurim BioCell Co. The ASCs were cultured in Dulbecco's Modified Eagle Medium (DMEM) with low glucose (GibcoBRL), supplemented with penicillin-streptomycin (GibcoBRL), and incubated at 37 °C in a humidified environment containing 5% CO_2.

Generation of PGC-1α–overexpressing adipose-derived stem cells

To create tASCs, ASCs were initially cultured in 100 mm cell dishes (Corning Glass Works) until they reached a confluence of 70%–80%. At this point, the ASCs were transiently transfected with 4 μg of pcDNA-PGC-1α, using a plasmid obtained from OriGene Technologies. After 24 hours after transfection, 5.0×10^5 ASCs were incubated in 10 mL of serum-free, low-glucose DMEM for another 24 hours.

Extracellular vesicles production

Conditioned medium was generated from 90% confluent ASC cultures that were maintained under starvation conditions (without fetal bovine serum) for 24 hours following transfection with 4 μg of pcDNA-PGC-1 for 24 hours. The conditioned medium was then collected and centrifuged at 2,500 ×*g* for 15 minutes at 4 °C to remove any cellular debris. An exosome isolation reagent was added to the conditioned medium, and the mixture was incubated overnight at 4 °C. The extracellular vesicles were isolated from the conditioned medium via differential centrifugation at 10,000 ×*g* for 60 minutes at 4 °C. After centrifugation, the extracellular vesicles were collected through standard centrifugation at 10,000 ×*g* for 60 minutes, and the resulting pellet was resuspended in phosphate-buffered saline (PBS).

Scaffold preparation

Porous cell supporting scaffolds, derived from serum proteins, were acquired from DaNAgreen Co., Ltd. These scaffolds were fabricated by aggregating proteins solubilized in bovine calf serum (Thermo 16170-078), crosslinking them into sheet forms, and subsequently cutting them into uniform sizes (Fig. 1A). Fig. 1B and C depict the surface morphologies of the scaffold as characterized by transmission electron microscopy and the cellular architecture post-seeding as revealed by H&E staining, respectively. For this experiment, disc-shaped scaffolds with a diameter of 10 mm and a thickness of 2 mm were utilized.

Real-time PCR

Total RNA was extracted from mouse liver tissue samples using TRIzol reagent (Invitrogen). For reverse transcription, 1 μg of RNA was used in conjunction with the RT-premix kit (TOYOBO) following the manufacturer's instructions. SYBR Green-based real-time quantitative PCR was then performed using specific primers: matrix metalloproteinase-2 (MMP-

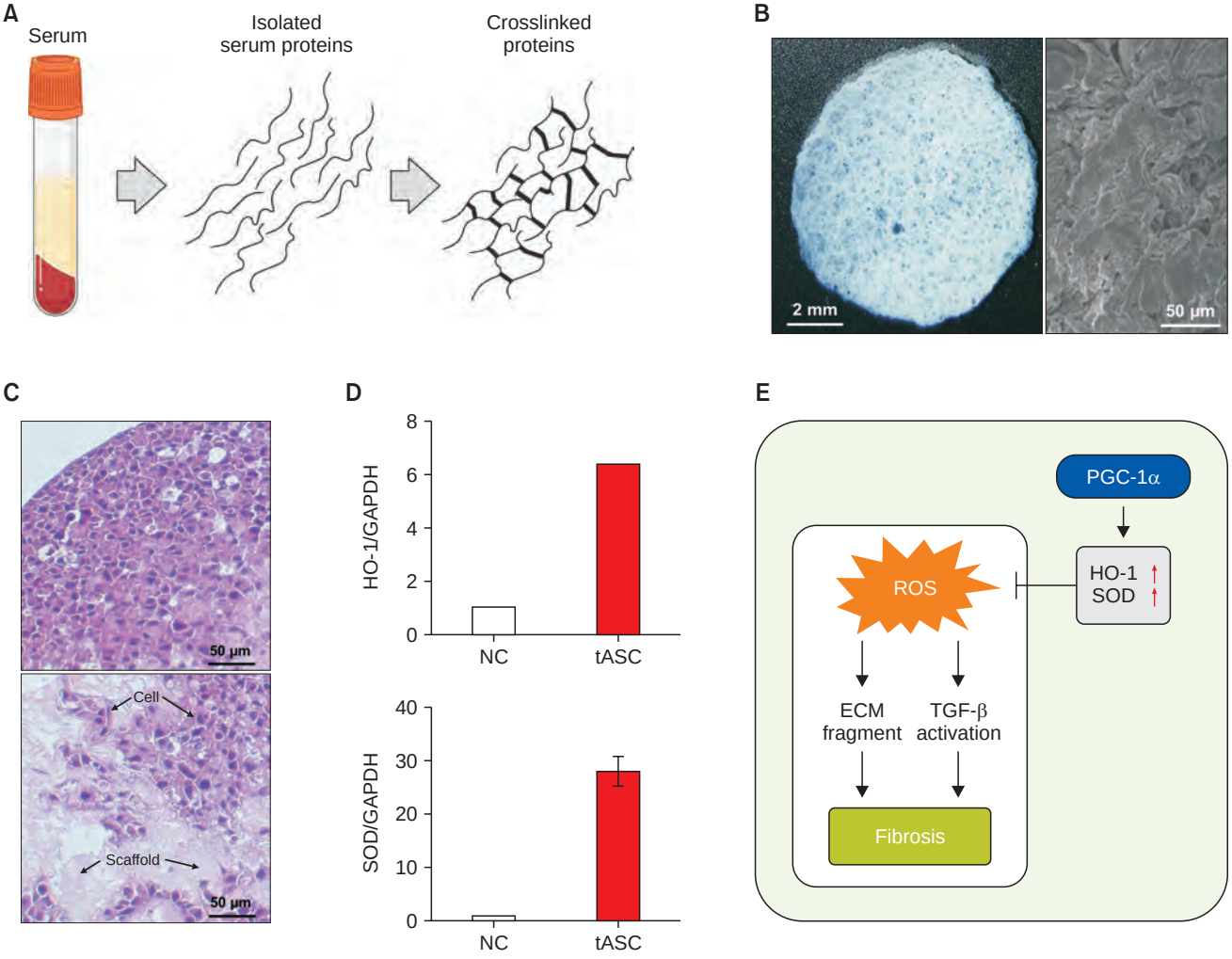

Fig. 1. Preparation of extracellular matrix (ECM) mimic scaffold. (A) ECM mimic scaffolds are fabricated by aggregating proteins solubilized in bovine calf serum, crosslinking them into sheet forms. (B) The surface morphologies of the Protinet (DaNAgreen) were examined using a scanning electron microscope (S-3000N, Hitachi), operated at an accelerating voltage of 5 kV. (C) The ECM mimic scaffold containing squamous cell carcinoma of the human cervix (SiHA) cells stained *en bloc* with H&E after formalin fixation and embedding in paraffin. One million SiHA cervical carcinoma cells were seeded on the 10-mm scaffold. SiHA cells were cultured in Dulbecco's Modified Eagle Medium containing 10% fetal bovine serum in a 5% CO_2 incubator for 14 days. (D) Real-time PCR results showing the expression levels of heme oxygenase-1 (HO-1) and superoxide dismutase (SOD) in peroxisome proliferator-activated receptor gamma coactivator 1-alpha (PGC-1α)–transfected ASCs (tASCs) compared to the normal control (NC). Both HO-1 and SOD are significantly upregulated in tASCs, suggesting an enhanced antioxidant capacity within these cells. (E) Schematic illustration of the potential mechanism through which PGC-1α alleviates fibrosis. PGC-1α upregulates the expression of HO-1 and SOD, leading to a reduction in reactive oxygen species (ROS) levels. This decrease in ROS inhibits fibrosis-related pathways, such as ECM and transforming growth factor-beta (TGF-β) fragment activation, ultimately contributing to the prevention of fibrosis. GAPDH, glyceraldehyde-3-phosphate dehydrogenase.

2; forward 5'-CAG GGA ATG AGT ACT GGG TC -3', reverse 5'-ACT CCA GTT AAA GGC AGC AT-3'); tissue inhibitor of metalloproteinases-1 (TIMP-1; forward 5'- GCA ACT CGG GCC TGG TCA TAA-3', reverse 5'- CGG CCC GTG ATG AGA AAC T-3'); mouse glyceraldehyde-3-phosphate dehydrogenase (GAPDH; forward 5'-CGA CTT CAA CAG CAA CTC CCA CTC TTC C-3', reverse 5'-TGG GTG GTC CAG GGT TTC TTA CTC CTT-3'); human PGC-1α (forward 5'-TCTCAGTACCCAGAACCATGCA-3', reverse 5'-GCTCCATGAATTCTCAGTCTTAACAA-3'); and human GAPDH (forward 5'-GCACCGTCAAGGCTGAGAAC-3', reverse 5'-TGGTGAAGACGCCAGTGGA-3'). These PCR reactions were conducted using the Applied Biosystems StepOnePlus real-time PCR system (Thermo).

ELISA

The concentrations of CD81 in ASCs were determined using a sandwich ELISA kit (Biolegend) following the manufacturer's protocol. Additionally, blood samples were collected from the mice and centrifuged at 3,000 ×*g* for 10 minutes. After centrifugation, the serum was isolated for further analysis.

Mouse interleukin 6 (IL-6) and tumor necrosis factor alpha (TNF-α) levels were also measured using the sandwich ELISA technique.

Western blot analysis

Mouse tissue samples were lysed using the EzRIPA Lysis Kit (ATTO Corp.), and protein concentrations were measured using the Bradford reagent (Bio-Rad). Specific immune complexes were detected with the Western Blotting Plus Chemiluminescence Reagent (Millipore). Primary antibodies against MMP-2 and alpha-smooth muscle actin (α-SMA) were sourced from Abcam, while TIMP-1 primary antibodies were purchased from Thermo Scientific. Primary antibodies against β-actin were obtained from Sigma Aldrich, and horseradish peroxidase-conjugated secondary antibodies were acquired from Vector Laboratories.

Immunohistochemistry and immunofluorescence

In the immunohistochemistry study, tissue sections that were formalin-fixed and paraffin-embedded were deparaffinized and rehydrated through a graded ethanol series. Epitope retrieval followed using established protocols. Antibodies against α-SMA and transforming growth factor-beta 1 (TGF-β1) were obtained from Abcam, and those for collagen type I alpha 1 were sourced from Santa Cruz Biotechnology. After staining, the samples were analyzed using a laser-scanning microscope (Eclipse TE300, Nikon) to assess the expression of these specific antibodies. For the immunofluorescence analysis, formalin-fixed and paraffin-embedded tissue sections were deparaffinized, rehydrated in an ethanol series, and subjected to epitope retrieval according to standard procedures. Antibodies against epithelial cell adhesion molecule (EpCAM) were used for immunofluorescence staining, with samples examined using a laser-scanning microscope (Eclipse TE300) to evaluate the expression of these antibodies.

Animals and study design

The animal experiments were carried out in accordance with the guidelines set by the Institute for Laboratory Animal Research at The Catholic University of Korea (No. CUMC-2020-0201-01). This study utilized 5-week-old male BALB/c mice, which were obtained from Orient Bio. The *in vivo* model involved creating hepatic fibrosis in mice through subcutaneous injections of thioacetamide (TAA) at a dosage of 200mg/kg, administered thrice weekly over a period of 5 weeks. An ECM mimic scaffold (Danagreen) was seeded with 5×10^5 tASCs and cultured in DMEM/low medium for 24 hours. The experiment was organized into 6 groups mainly categorized by the mice's liver condition being either fibrotic or non-fibrotic. Non-fibrotic mice received either intravenous normal saline (Nor-Nsal, n = 10), intravenous tASCs (Nor-Cell, n = 10), or implantation of tASCs-containing scaffolds (Nor-Scaf, n = 10). Likewise, fibrotic mice were treated with intravenous normal saline (Fib-Nsal, n = 10), intravenous tASCs (Fib-Cell, n = 10), or scaffold implantation with tASCs (Fib-Scaf, n = 10). For the Cell groups (Nor-Cell and Fib-Cell), 5×10^5 tASCs in 100 μL PBS were injected twice weekly for 4 weeks through the tail vein. In the Scaf groups (Nor-Scaf and Fib-Scaf), a scaffold containing 5×10^5 tASCs was implanted in the flank region and maintained for the same duration. Specifically, scaffold implantation was conducted under anesthesia induced by intraperitoneal injection of Zoletil (30 mg/kg, Virbac) and Rompun (10 mg/kg, Elanco). The right thigh region of the mouse was shaved, and the mouse was positioned on its back. A lateral incision of approximately 1 cm was made in the subcutaneous tissue above the right thigh, where a membrane pouch containing the scaffold was inserted, followed by suturing. Four weeks after implantation, mice were euthanized to assess the treatment effects.

Statistical analysis

The data analysis was performed using SPSS ver. 11.0 (SPSS Inc.), with results expressed as mean ± standard deviation. Statistical comparisons between groups were conducted using the Kruskal-Wallis test. A P-value of less than 0.05 was considered to indicate statistical significance.

RESULTS

Establishment of PGC-1α–overexpressing adipose-derived stem cells–containing scaffold implantation

After generating tASCs, their characteristics were assessed by real-time PCR. The expression of key antioxidant enzymes, heme oxygenase-1 (HO-1) and superoxide dismutase (SOD), was significantly upregulated in PGC-1α–transfected ASCs compared to the normal control cells ($P < 0.05$) (Fig. 1D). This indicates that PGC-1α overexpression enhances the antioxidant capacity of ASCs. It is well established that PGC-1α overexpression can support antifibrotic processes by upregulating antioxidant enzymes [9,10] (Fig. 1E). Specifically, PGC-1α induces the expression of enzymes like HO-1 and SOD, which reduce the accumulation of reactive oxygen species (ROS). Since ROS play a pivotal role in promoting fibrosis through the activation of ECM fragments and TGF-β signaling, their suppression by PGC-1α–driven antioxidant activity inhibits the progression of fibrosis. This mechanism underscores the antifibrotic potential of tASCs.

The antifibrogenic effects of transfected ASCs were compared between 2 methods of administration: intravenous injection and scaffold implantation in the subcutaneous region. Fig. 2A provides a brief description of the experiment. Initially, PGC-1α was transfected into ASCs to produce tASCs. These tASCs were then transferred to the ECM mimic scaffold and cultured for

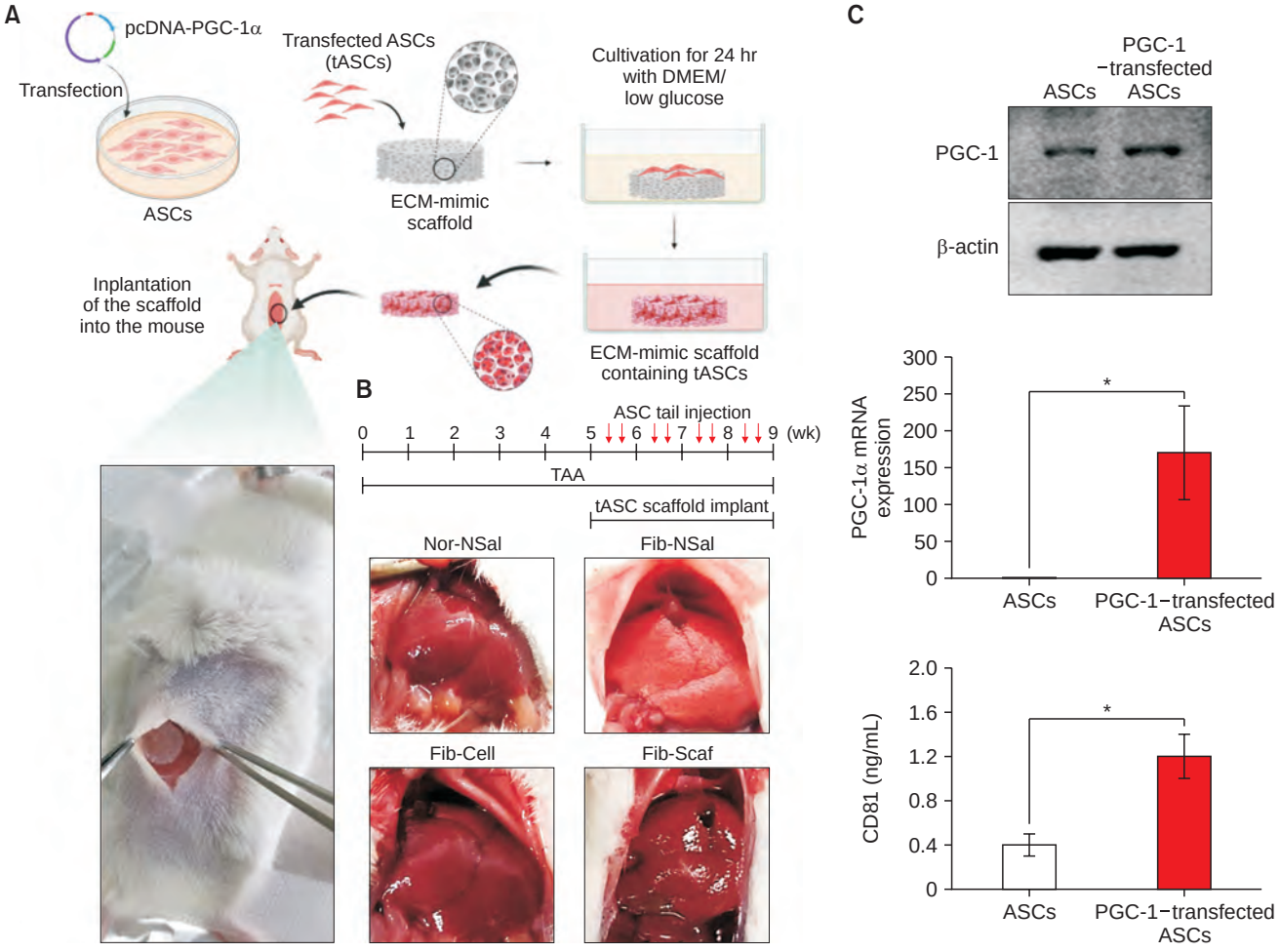

Fig. 2. Comparative analysis of antifibrogenic effects in liver fibrosis model treated with PGC-1α–modified ASCs. (A) Schematic representation of the experimental design detailing the generation and implantation of a scaffold containing PGC-1α–overexpressing ASCs (tASCs). (B) Macroscopic examination of liver tissues posttreatment. The livers in the thioacetamide (TAA)-treated control group (Fib-Nsal) show evident fibrotic alterations with nodularity and varied coloration, contrasted with the markedly improved appearance in both Fib-Cell and Fib-Scaf groups, demonstrating substantial fibrosis mitigation. (C) Verification of the successful transfection of PGC-1 into ASCs and its effect. Western blot (left) shows elevated PGC-1 protein levels in plasmid containing DNA (pcDNA)-PGC-1α–transfected ASCs. Real-time PCR analysis (middle) confirms increased PGC-1 messenger RNA (mRNA) expression. ELISA results (right) indicate a threefold rise in CD81-marked exosome levels in the transfected ASCs compared to controls, suggesting an enhanced regenerative profile. The relative densities of the individual markers were quantified using the Image J software (National Institutes of Health). Data are expressed as mean ± standard deviation based on 3 separate experiments. PGC-1α, peroxisome proliferator-activated receptor gamma coactivator 1-alpha; ASC, adipose-derived stem cell; pcDNA, plasmid containing DNA; DMEM, Dulbecco's Modified Eagle Medium; ECM, extracellular matrix. *$P < 0.05$.

24 hours in DMEM with low glucose. Subsequently, scaffolds embedded with tASCs were implanted into the subcutaneous area in a liver fibrosis mouse model (Fib-Scaf group). In a parallel protocol, an equivalent number of tASCs were intravenously injected into a separate group of liver fibrosis mice (Fib-Cell group), with treatments administered twice per week for 4 weeks.

Four weeks after treatment, upon laparotomy, the gross appearance of the liver was compared across groups (Fig. 2B). In the TAA-treated Fib-Nsal group, livers exhibited irregular surface nodularity, a spectrum of coloration from pale to dark areas, and a texture firmer and less pliable than normal liver tissue, indicative of fibrotic changes. However, in the treatment groups (Fib-Cell and Fib-Scaf), these characteristics were markedly ameliorated, with the liver's gross appearance nearly indistinguishable from that of the control liver, suggesting significant recovery. No discernible differences in gross appearance were observed between the Fib-Cell and Fib-Scaf groups.

To verify successful transfection of pc-DNA-PGC-1 into ASCs, Western blot analysis was conducted, revealing an elevation in PGC-1 protein levels (Fig. 2C, left). Real-time PCR corroborated

this finding at the transcriptional level (Fig. 2C, middle). Following transfection, exosomes isolated from the culture media, marked by CD81, were found to increase approximately threefold in PGC-1–transfected ASCs relative to controls, as quantified by ELISA (Fig. 2C, right). This augmentation in exosome production implies a potential enhancement in the regenerative factor profile of PGC-1 modified ASCs, aligning with the recognized significance of stem cell-derived exosomes in tissue regeneration processes.

Molecular determination of fibrosis

The expression levels of fibrosis-associated markers in liver tissues post-treatment were evaluated using real-time PCR (Fig. 3A). In normal (non-fibrotic) mice, no significant changes were

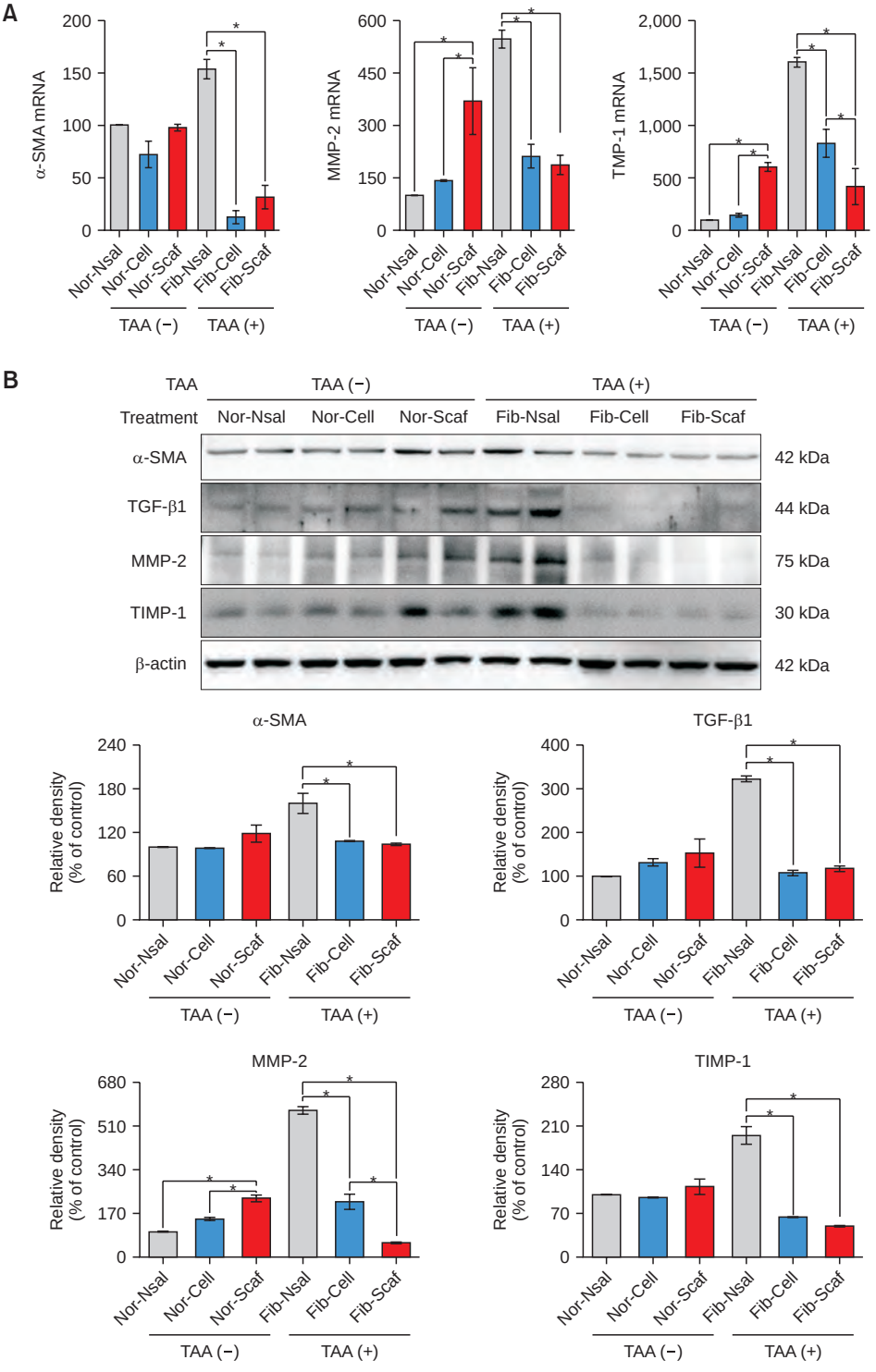

Fig. 3. Molecular analysis of fibrosis-related markers in liver tissues after treatment. (A) Real-time PCR results for fibrosis markers. Both the Fib-Cell and Fib-Scaf groups demonstrated a significant reduction in messenger RNA (mRNA) levels of the profibrotic markers alpha-smooth muscle actin (α-SMA) and matrix metalloproteinase-2 (MMP-2), as compared to the control group (Fib-Nsal). The expression of the antifibrotic marker tissue inhibitor of metalloproteinases-1 (TIMP-1) was also significantly lower in the treatment groups, particularly in the Fib-Scaf group, than in the control. (B) Western blot results for fibrosis markers. The Fib-Cell and Fib-Scaf groups exhibited reduced levels of profibrotic markers α-SMA and transforming growth factor-beta 1 (TGF-β1), with a notably significant reduction in MMP-2 within the Fib-Scaf group. The antifibrotic marker TIMP-1 was also considerably reduced in the treatment groups when compared to controls. The relative densities of each marker were quantified using Image J software (National Institutes of Health) and normalized to β-actin levels in each group. Results are expressed as mean ± standard deviation across 3 independent experiments. TAA, thioacetamide. *P < 0.05.

observed in the expression of the profibrotic marker α-SMA across the groups. However, in the Nor-Scaf group, there was a significant increase in the messenger RNA (mRNA) levels of the profibrotic marker MMP-2 and the antifibrotic marker TIMP-1 ($P < 0.05$). In TAA-treated mice, the Fib-Cell and Fib-Scaf groups exhibited markedly lower mRNA expression of the profibrotic markers α-SMA and MMP-2 compared to the control group (Fib-Nsal) ($P < 0.05$), with no significant difference between the 2 treated groups. Additionally, in the fibrosis model, the mRNA levels of the antifibrotic marker TIMP-1 were significantly reduced in both treatment groups (Fib-Cell and Fib-Scaf) compared to the control (Fib-Nsal), with the most substantial reduction observed in the Fib-Scaf group ($P < 0.05$).

Further analysis included Western blotting of liver tissues from each group to assess the expression levels of fibrosis-associated markers (Fig. 3B). In non-fibrotic (normal) liver mice, only minor differences in the expression of these markers were observed between the groups. However, in TAA-treated mice, the Fib-Cell and Fib-Scaf groups exhibited significantly lower expression of the profibrotic markers α-SMA and TGF-β1 compared to the control group (Fib-Nsal) ($P < 0.05$), with no significant variation between the 2 treated groups. MMP-2 expression showed a more pronounced decrease in the treatment groups (Fib-Cell and Fib-Scaf) relative to Fib-Nsal, with the most marked reduction observed in the Fib-Scaf group ($P < 0.05$). Additionally, the antifibrotic marker TIMP-1 was significantly lower in the treatment groups compared to the Fib-Nsal group ($P < 0.05$). Overall, both intravenous and scaffold-based delivery of tASCs demonstrated antifibrotic effects in the mouse fibrosis model, with molecular analyses indicating no significant differences between the 2 treatment groups.

Comparison of serum systemic inflammatory markers and liver enzymes

Four weeks after treatment, blood was collected from mice in each group for ELISA to evaluate changes in serum inflammatory markers (Fig. 4A). In TAA-treated mice, the Fib-Cell and Fib-Scaf groups showed a significant decrease in serum levels of TNF-α and IL-6 compared to the Fib-Nsal control group ($P < 0.05$). No significant differences were observed between the Fib-Cell and Fib-Scaf groups regarding these inflammatory markers. Subsequently, liver enzyme levels were assessed using blood samples collected 4 weeks after treatment (Fig. 4B). The Fib-Cell group demonstrated significantly reduced AST levels, while the Fib-Scaf group exhibited significantly lower levels of both AST and ALT compared to the control group (Fib-Nsal) ($P < 0.05$). No significant differences in AST and ALT levels were found between the Fib-Cell and Fib-Scaf groups. In conclusion, both intravenous administration and scaffold implantation of tASCs in the fibrosis mouse model exhibited anti-inflammatory effects and effectively reduced elevated liver enzymes. No significant differences were noted in these effects between the 2 treatment groups.

Histological determination of fibrosis

Four weeks after treatment, liver tissues were collected from

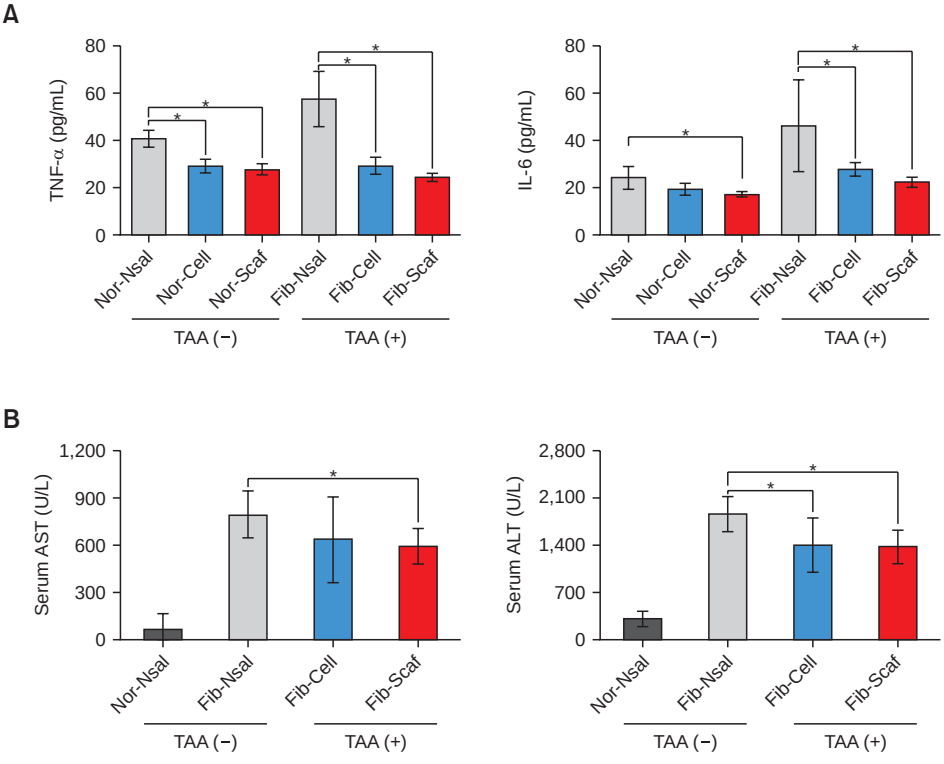

Fig. 4. Analysis of systemic serum inflammatory markers and liver enzymes. (A) ELISA data showing the comparison of serum inflammatory marker levels. In thioacetamide (TAA)-treated mice, both the Fib-Cell and Fib-Scaf groups exhibited significant reductions in tumor necrosis factor alpha (TNF-α) and interleukin 6 (IL-6) levels compared to the control group (Fib-Nsal), with no noticeable differences between the 2 groups. (B) Comparison of serum liver enzyme levels (AST and ALT) across groups. The Fib-Cell group presented significantly reduced AST levels, while the Fib-Scaf group showed lower levels of both AST and ALT compared to the control (Fib-Nsal) ($P < 0.05$), with no significant differences between the 2 experimental groups. Data are expressed as mean ± standard deviation from 3 independent experiments. *$P < 0.05$.

each group, and various staining techniques were used to examine the effects of the treatments on liver tissues (Fig. 5A). H&E staining was initially performed, followed by the evaluation of fibrosis severity using the Ishak score. A comparison of Ishak scores showed a significant reduction in fibrosis in both the Fib-Cell and Fib-Scaf groups compared to the Fib-Nsal control group. Moreover, the Fib-Scaf group demonstrated a more pronounced decrease in the Ishak score than the Fib-Cell group ($P < 0.05$). Subsequently, Masson's trichrome staining was used to further assess the extent of fibrosis among the groups (Fig. 5B). Based on Masson's trichrome staining results, the Fib-Cell group did not exhibit a significant reduction in fibrosis scores compared to Fib-Nsal, while the Fib-Scaf group showed a significant decrease in fibrosis scores compared to both the Fib-Nsal and Fib-Cell groups ($P < 0.05$).

Finally, immunohistochemical staining was used to compare the expression of fibrosis-related markers in each group. Immunohistochemical staining for profibrotic markers, including α-SMA, collagen type I alpha, and TGF-β1 was conducted (Fig. 6). In each staining, both treatment groups (Fib-Cell and Fib-Scaf) exhibited significantly lower immunoreactivity compared to the Fib-Nsal group ($P < 0.05$). Moreover, the Fib-Scaf group demonstrated significantly lower immunoreactivity than the Fib-Cell group ($P < 0.05$), highlighting its superior antifibrotic efficacy. Collectively, all histological evaluations indicate that scaffold implantation of tASCs exhibits a higher antifibrogenic effect compared to intravenous administration. Integrating these findings with molecular studies, it can be inferred that scaffold-based cell therapy potentially has a higher or at least equivalent antifibrogenic effect compared to cell therapy alone.

To assess stem cell distribution within the liver following 4 weeks of treatment, the expression levels of EpCAM, a marker prominently expressed in hepatocytes and hepatic cancer stem cells, were evaluated via immunofluorescent staining of liver tissues. The treatment groups, both Fib-Cell and Fib-Scaf, exhibited a significant elevation in EpCAM expression when compared to controls ($P < 0.05$). Notably, the Fib-Scaf group demonstrated a markedly higher expression of EpCAM than the Fib-Cell group ($P < 0.05$). This indicates a superior distribution and engraftment efficiency of stem cells delivered using the scaffold-based method (Supplementary Fig. 1), suggesting its

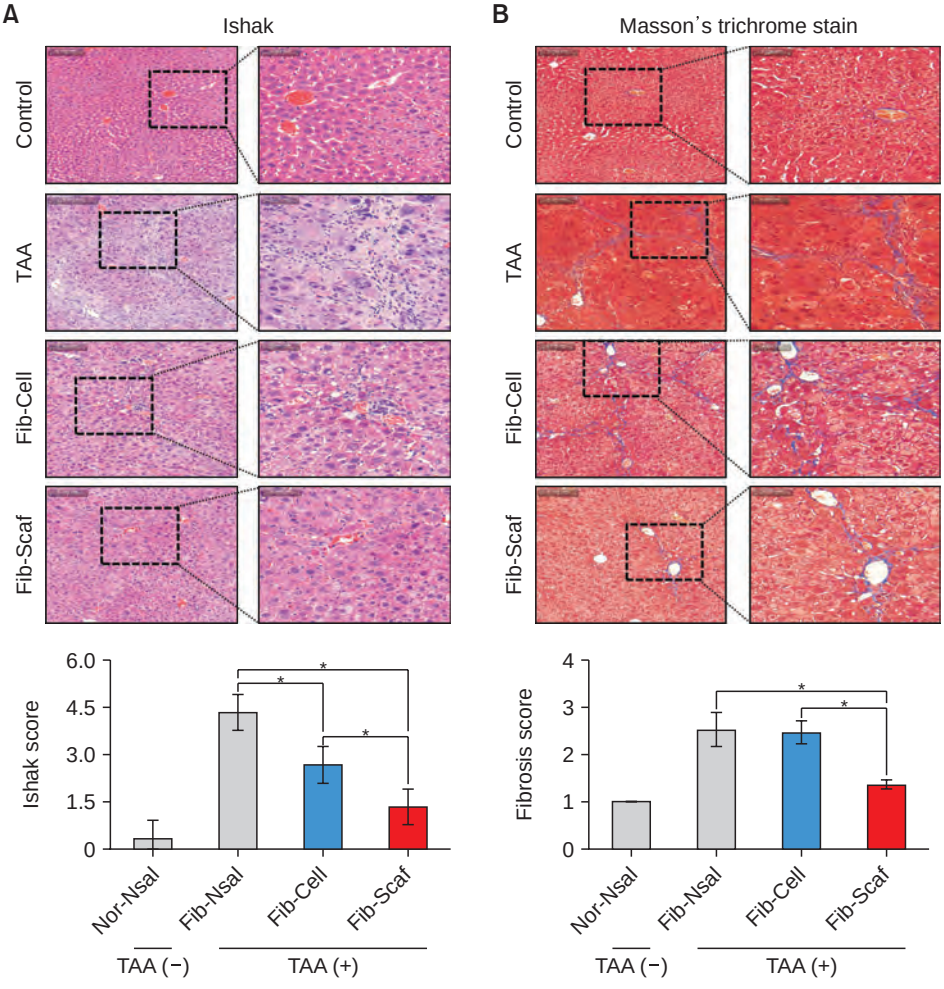

Fig. 5. Histological analysis of liver tissues post-treatment. (A) H&E staining and Ishak score assessment. The Ishak score, used to evaluate fibrosis degree, shows a significant decrease in both Fib-Cell and Fib-Scaf groups compared to the control (Fib-Nsal), with a more notable reduction in the Fib-Scaf group. (B) Masson's trichrome staining for fibrosis evaluation. While the Fib-Cell group's fibrosis score did not significantly differ from the control, the Fib-Scaf group exhibited a marked reduction in fibrosis, outperforming both the control and the Fib-Cell group. TAA, thioacetamide. *$P < 0.05$.

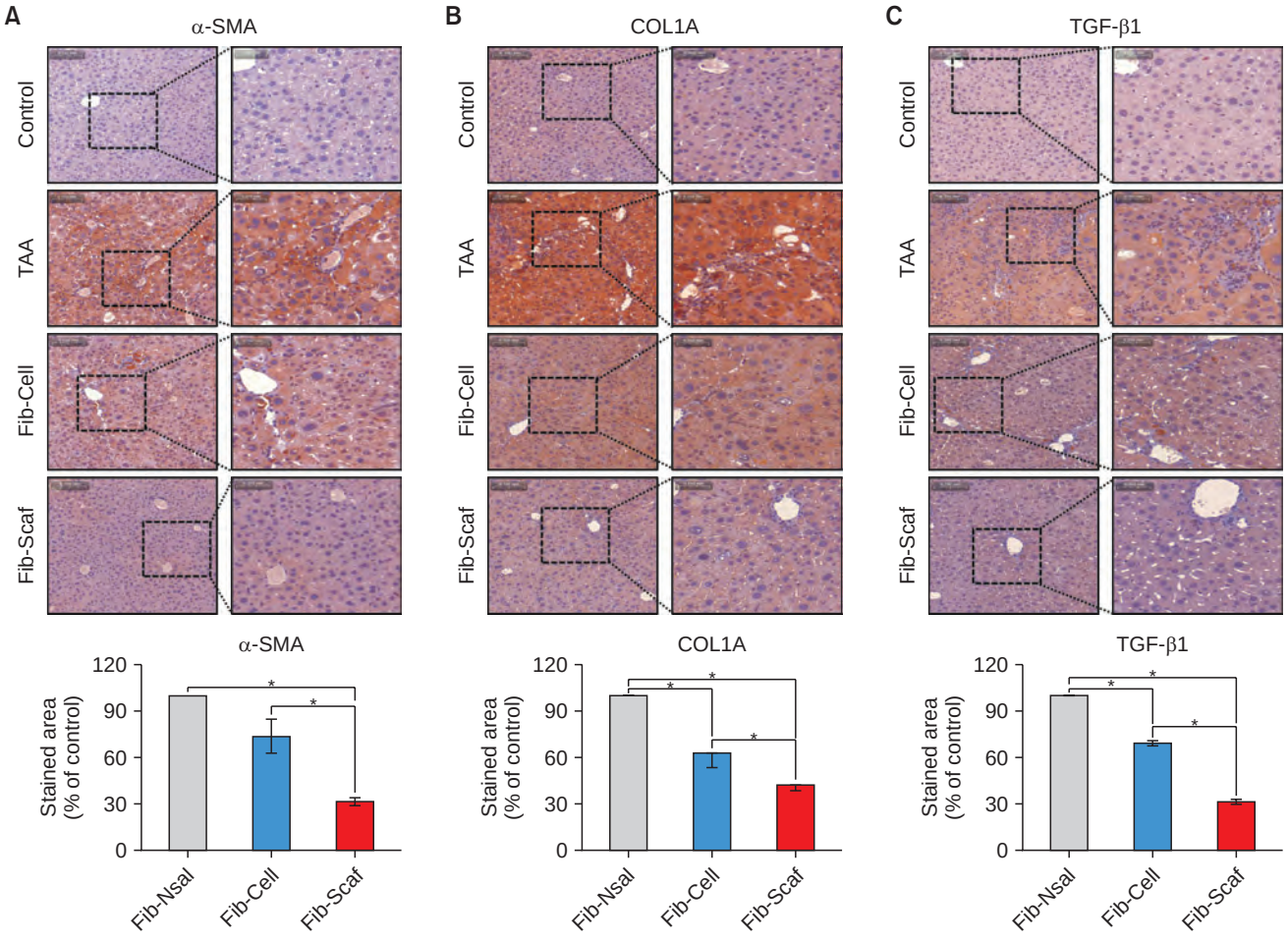

Fig. 6. Immunohistochemical assessment of markers associated with fibrosis. (A) Alpha-smooth muscle actin (α-SMA) staining. Fib-Scaf showed the most pronounced decrease in α-SMA immunoreactivity. (B) Collagen type I alpha (COL1A) staining. Similar to α-SMA, Fib-Scaf demonstrated the greatest reduction in COL1A immunoreactivity. (C) Transforming growth factor-beta 1 (TGF-β1) staining. Once again, Fib-Scaf presented the largest decrease in TGF-β1 immunoreactivity, reflecting its strong antifibrotic potential. Data are reported as mean ± standard deviation from 3 separate experiments. Immunoreactive areas were quantified using Image J software (National Institutes of Health) and are expressed as relative percentages compared to control samples. TAA, thioacetamide. *P < 0.05.

potential for enhanced liver regeneration.

DISCUSSION

This study assessed the antifibrogenic effects of tASCs in a liver fibrosis mouse model, focusing on 2 methods of delivery: intravenous injection and scaffold implantation. Molecular analysis revealed that both methods significantly reduced the expression of fibrotic markers (α-SMA, MMP-2, TGF-β1) and inflammatory markers (TNF-α, IL-6) compared to controls, with no significant difference between each other [1,11]. Histological assessments using H&E and Masson's trichrome staining, as well as immunohistochemical staining for profibrotic markers, showed that the scaffold implantation group (Fib-Scaf) had a more pronounced reduction in fibrosis and lower immunoreactivity for fibrotic markers than the intravenous group (Fib-Cell), indicating a superior antifibrogenic effect. Overall, scaffold-based delivery of tASCs was found to be potentially more effective or at least equivalent in antifibrogenic activity compared to intravenous delivery in this fibrosis model.

Of all the kinds of scaffolds, biological scaffolds of liver were utilized in this study. These scaffolds, based on the ECM, are gaining importance in regenerative medicine for their ability to create an ideal environment for cell growth [12,13]. Reconstructing ECM mimic scaffolds results in a 3-dimensional, acellular scaffold that maintains the specific structural features and bioactive elements of the organ, encompassing both macro and micro aspects [14]. The ECM, a secretion of organ-specific resident cells, emerges as an optimal scaffold for subsequent cell repopulation [15]. Its composition includes a variety of extracellular macromolecules like collagen, elastin, laminin, glycosaminoglycans, and fibronectin, each

present in varying concentrations, providing crucial structural and biochemical support to the cells in its vicinity [16]. ECM facilitates interactions between cells, adherence of cells to the matrix, and the differentiation of progenitor cells in a location-specific manner [17,18]. Furthermore, ECM-based scaffolds are instrumental in guiding cell migration, proliferation, and differentiation [14]. Liver ECM scaffolds were found to retain essential growth factors like vascular endothelial growth factors, hepatocyte growth factors, and epithelial growth factors, crucial for hepatocyte differentiation and function [19,20].

This study employed tASCs for both intravenous administration and scaffold implantation, given the pivotal role of PGC-1α in liver fibrosis development, particularly its influence on energy metabolism and mitochondrial function [21,22]. As a key regulator of energy balance, PGC-1α plays a crucial role in preventing the onset of metabolic syndrome and the mitochondrial dysfunction associated with nonalcoholic fatty liver disease (NAFLD) [23-25]. This dysfunction is characterized by increased mitochondrial fission and reduced fusion, which impairs mitochondrial integrity and function. In the context of NAFLD, mitochondrial dysfunction is central to its pathogenesis, with PGC-1α functioning as an important regulator of lipid metabolism. PGC-1α specifically binds to the nuclear receptor peroxisome proliferator-activated receptor alpha, which is crucial for the liver's adaptation to fasting, playing an essential role in beta-oxidation [26]. Reduced PGC-1α activity and impaired mitochondrial biogenesis have been linked to NAFLD in mouse models. Mice with liver-specific PGC-1α deletion show signs of hepatic steatosis, partly due to reduced mitochondrial oxidative capacity and dysfunction [27]. Conversely, hepatic overexpression of PGC-1α enhances fatty acid oxidation, which leads to lower triglyceride storage [28]. This regulation of mitochondrial dynamics by PGC-1α highlights its essential role in the progression from hepatic steatosis to NASH and subsequent fibrosis [23-25,29].

This research indicated that TIMP-1, a known antifibrotic marker, was significantly elevated in a liver fibrosis model prior to treatment and exhibited a decrease in levels following the treatment. In the context of liver fibrosis, the observed decrease in profibrogenic markers such as MMP-2 and α-SMA, along with the initially high levels of the antifibrotic marker TIMP-1 in untreated groups and their subsequent reduction following treatment, can be explained by the role of TIMPs in liver fibrosis. TIMPs are known to promote pro-survival signals in activated hepatic stellate cells (HSCs) and to activate nuclear factor kappa B, which mediates the survival of activated HSCs via the upregulation of B-cell lymphoma 2 (BCL2) and downregulation of proapoptotic factors like BCL2-associated X protein, p53 upregulated modulator of apoptosis, and p53 [30]. Therefore, the high TIMP-1 expression in untreated groups could be attributed to its role in maintaining the survival of activated HSCs, which are key players in liver fibrosis [31]. Following treatment, as the profibrogenic activity reduces due to the decrease in MMP-2 and α-SMA, the need for TIMP-1–mediated survival signals in HSCs diminishes, leading to its reduction [32]. This shift suggests an effective therapeutic intervention that not only suppresses profibrogenic markers but also reduces the survival signals in HSCs, facilitating the regression of liver fibrosis.

In conclusion, this research showed that tASCs, whether administered through scaffold implantation or intravenous injection, effectively reduced fibrosis in a liver fibrosis mouse model. Upon integrating molecular studies and histological evaluations, it was observed that ASCs delivered via scaffold implantation provided superior or at least equivalent antifibrotic efficacy compared to intravenous delivery. Additionally, scaffold-implanted ASCs demonstrated comparable systemic anti-inflammatory effects and effectiveness in reducing elevated liver enzymes to those achieved by intravenous delivery. In clinical settings, scaffold implantation involves operative or procedural interventions as a drawback, while intravenous delivery requires the inconvenience of frequent administrations. Considering their efficacy, scaffold implantation presents as an advantageous alternative for patients looking to avoid the difficulties or frequent nature of intravenous treatments.

SUPPLEMENTARY MATERIALS

Supplementary Fig. 1 can be found via https://doi.org/10.4174/astr.2025.108.3.186.

ACKNOWLEDGEMENTS

We would like to extend our sincere thanks to Jeong-Yeon Seo for assistance with manuscript preparation and to Jennifer Lee for her contributions to the illustration work.

Fund/Grant Support

This study was supported by the Research Fund of The Catholic University of Korea, Seoul St. Mary's Hospital (No. ZC19CISI0673).

Conflict of Interest

No potential conflict of interest relevant to this article was reported.

ORCID iD

Joseph Ahn: https://orcid.org/0000-0001-8528-4919
Jung Hyun Park: https://orcid.org/0000-0003-2693-0655
Ho Joong Choi: https://orcid.org/0000-0002-0862-098X
Dosang Lee: https://orcid.org/0000-0002-1528-2317

Ha-Eun Hong: https://orcid.org/0000-0002-4361-4809
Ok-Hee Kim: https://orcid.org/0000-0002-9204-2587
Say-June Kim: https://orcid.org/0000-0001-5171-4837

Author Contribution

Conceptualization: JA, JHP, SJK
Formal Analysis: HJC
Investigation: JA, OHK
Methodology: SJK, HEH, OHK
Project Administration: DL, JHP, HJC
Writing – Original Draft: JA
Writing – Review & Editing: All authors

REFERENCES

1. Abdel-Rahman RF, Fayed HM, Asaad GF, Ogaly HA, Hessin AF, Salama AA, et al. The involvement of TGF-β1 /FAK/ α-SMA pathway in the antifibrotic impact of rice bran oil on thioacetamide-induced liver fibrosis in rats. PLoS One 2021;16:e0260130.
2. Cardinale V, Lanthier N, Baptista PM, Carpino G, Carnevale G, Orlando G, et al. Cell transplantation-based regenerative medicine in liver diseases. Stem Cell Reports 2023;18:1555-72.
3. Huai Q, Zhu C, Zhang X, Dai H, Li X, Wang H. Mesenchymal stromal/stem cells and their extracellular vesicles in liver diseases: insights on their immunomodulatory roles and clinical applications. Cell Biosci 2023;13:162.
4. Dwyer BJ, Macmillan MT, Brennan PN, Forbes SJ. Cell therapy for advanced liver diseases: repair or rebuild. J Hepatol 2021;74:185-99.
5. Habeeb MA, Vishwakarma SK, Bardia A, Khan AA. Hepatic stem cells: a viable approach for the treatment of liver cirrhosis. World J Stem Cells 2015;7:859-65.
6. Ogasawara H, Inagaki A, Fathi I, Imura T, Yamana H, Saitoh Y, et al. Preferable transplant site for hepatocyte transplantation in a rat model. Cell Transplant 2021;30:9636897211040012.
7. Chawla S, Das A. Preclinical-to-clinical innovations in stem cell therapies for liver regeneration. Curr Res Transl Med 2023;71:103365.
8. Jiang WC, Cheng YH, Yen MH, Chang Y, Yang VW, Lee OK. Cryo-chemical decellularization of the whole liver for mesenchymal stem cells-based functional hepatic tissue engineering. Biomaterials 2014;35:3607-17.
9. Cheng CF, Ku HC, Lin H. PGC-1α as a pivotal factor in lipid and metabolic regulation. Int J Mol Sci 2018;19:3447.
10. Abu Shelbayeh O, Arroum T, Morris S, Busch KB. PGC-1α is a master regulator of mitochondrial lifecycle and ROS stress response. Antioxidants (Basel) 2023;12:1075.
11. Kim KH, Lee JI, Kim OH, Hong HE, Kwak BJ, Choi HJ, et al. Ameliorating liver fibrosis in an animal model using the secretome released from miR-122-transfected adipose-derived stem cells. World J Stem Cells 2019;11:990-1004.
12. Faulk DM, Carruthers CA, Warner HJ, Kramer CR, Reing JE, Zhang L, et al. The effect of detergents on the basement membrane complex of a biologic scaffold material. Acta Biomater 2014;10:183-93.
13. Ott HC, Matthiesen TS, Goh SK, Black LD, Kren SM, Netoff TI, et al. Perfusion-decellularized matrix: using nature's platform to engineer a bioartificial heart. Nat Med 2008;14:213-21.
14. Crapo PM, Gilbert TW, Badylak SF. An overview of tissue and whole organ decellularization processes. Biomaterials 2011;32:3233-43.
15. Brown BN, Badylak SF. Extracellular matrix as an inductive scaffold for functional tissue reconstruction. Transl Res 2014;163:268-85.
16. Walker C, Mojares E, Del Río Hernández A. Role of extracellular matrix in development and cancer progression. Int J Mol Sci 2018;19:3028.
17. Evans DW, Moran EC, Baptista PM, Soker S, Sparks JL. Scale-dependent mechanical properties of native and decellularized liver tissue. Biomech Model Mechanobiol 2013;12:569-80.
18. Sánchez-Romero N, Sainz-Arnal P, Pla-Palacín I, Dachary PR, Almeida H, Pastor C, et al. The role of extracellular matrix on liver stem cell fate: a dynamic relationship in health and disease. Differentiation 2019;106:49-56.
19. Jaramillo M, Yeh H, Yarmush ML, Uygun BE. Decellularized human liver extracellular matrix (hDLM)-mediated hepatic differentiation of human induced pluripotent stem cells (hIPSCs). J Tissue Eng Regen Med 2018;12:e1962-73.
20. Uygun BE, Soto-Gutierrez A, Yagi H, Izamis ML, Guzzardi MA, Shulman C, et al. Organ reengineering through development of a transplantable recellularized liver graft using decellularized liver matrix. Nat Med 2010;16:814-20.
21. Jiang Y, Chen D, Gong Q, Xu Q, Pan D, Lu F, et al. Elucidation of SIRT-1/PGC-1α-associated mitochondrial dysfunction and autophagy in nonalcoholic fatty liver disease. Lipids Health Dis 2021;20:40.
22. Garcia S, Nissanka N, Mareco EA, Rossi S, Peralta S, Diaz F, et al. Overexpression of PGC-1α in aging muscle enhances a subset of young-like molecular patterns. Aging Cell 2018;17:e12707.
23. Lin J, Handschin C, Spiegelman BM. Metabolic control through the PGC-1 family of transcription coactivators. Cell Metab 2005;1:361-70.
24. Raffaele M, Bellner L, Singh SP, Favero G, Rezzani R, Rodella LF, et al. Epoxyeico-

satrienoic intervention improves NAFLD in leptin receptor deficient mice by an increase in PGC1α-HO-1-PGC1α-mitochondrial signaling. Exp Cell Res 2019;380:180-7.
25. Singh SP, Schragenheim J, Cao J, Falck JR, Abraham NG, Bellner L. PGC-1 alpha regulates HO-1 expression, mitochondrial dynamics and biogenesis: role of epoxyeicosatrienoic acid. Prostaglandins Other Lipid Mediat 2016;125:8-18.
26. Gao D, Nong S, Huang X, Lu Y, Zhao H, Lin Y, et al. The effects of palmitate on hepatic insulin resistance are mediated by NADPH Oxidase 3-derived reactive oxygen species through JNK and p38MAPK pathways. J Biol Chem 2010;285:29965-73.
27. Sommer J, Mahli A, Freese K, Schiergens TS, Kuecuekoktay FS, Teufel A, et al. Analysis of molecular mechanisms of 5-fluorouracil-induced steatosis and inflammation in vitro and in mice. Oncotarget 2017;8:13059-72.
28. Morris EM, Meers GM, Booth FW, Fritsche KL, Hardin CD, Thyfault JP, et al. PGC-1α overexpression results in increased hepatic fatty acid oxidation with reduced triacylglycerol accumulation and secretion. Am J Physiol Gastrointest Liver Physiol 2012;303:G979-92.
29. Sacerdoti D, Singh SP, Schragenheim J, Bellner L, Vanella L, Raffaele M, et al. Development of NASH in obese mice is confounded by adipose tissue increase in inflammatory NOV and oxidative stress. Int J Hepatol 2018;2018:3484107.
30. Kisseleva T, Brenner D. Molecular and cellular mechanisms of liver fibrosis and its regression. Nat Rev Gastroenterol Hepatol 2021;18:151-66.
31. Parsons CJ, Bradford BU, Pan CQ, Cheung E, Schauer M, Knorr A, et al. Antifibrotic effects of a tissue inhibitor of metalloproteinase-1 antibody on established liver fibrosis in rats. Hepatology 2004;40:1106-15.
32. Murphy FR, Issa R, Zhou X, Ratnarajah S, Nagase H, Arthur MJ, et al. Inhibition of apoptosis of activated hepatic stellate cells by tissue inhibitor of metalloproteinase-1 is mediated via effects on matrix metalloproteinase inhibition: implications for reversibility of liver fibrosis. J Biol Chem 2002;277:11069-76.